First publ. in: High magnetic fields / ed. by Fritz Herlach ... 2. Theory and experiments I, Singapore, World Scientific, 2003

HIGH MAGNETIC FIELDS IN CHEMISTRY

U. E. STEINER
Fakultät für Chemie, Universität Konstanz,
D-78457 Konstanz, Germany, E-mail: ulrich.steiner@uni-konstanz.de

P. GILCH
Sektion Physik, Oettingenstr. 67, Ludwig-Maximilians-Universität, D-80538 München, Germany
E-mail: peter.gilch@physik.uni-muenchen.de

Recent applications of large ($\sim$ 1 T – $\sim$ 30 T) magnetic fields in modern chemical research are reviewed. Magnetic field effects of chemical relevance appear on the levels of quantum mechanics, thermodynamics, and macroscopic forces. Quantum mechanical magnetic field effects are governed by the Zeeman interaction and are borne out as static and dynamic effects in spectroscopy and in chemical kinetics. Magnetic circular dichroism (MCD) spectroscopy and magnetic fluorescence quenching in the gas phase serve to illustrate the former, while radical pair spin chemistry is representative of the latter. The principles of the radical pair mechanism are outlined and high-field applications are illustrated in some detail for photo-induced electron transfer reactions of some transition metal complexes. Thermodynamic effects concern the magnetization of chemical samples, which is the focus of magnetochemistry or — more modern — molecular magnetism, and the equilibrium of chemical reactions. Representative examples of both aspects are described. Finally, the exploitation of orientational forces caused by the magnetic anisotropy of larger particles (from macromolecules to micro-crystals) is exemplified. Crystal growth in a magnetic field may hold a potential for achieving better control of the quality of protein crystals for structural analysis.

1 Introduction

Magnetic effects that are of interest in chemistry may be classified into one of the following categories[a]:

1. Zeeman effects (quantum mechanics)
2. Equilibrium (thermodynamics)
3. Macroscopic forces (classical mechanics)

The first group is concerned with the energetic effects of the interactions between magnetic fields and the magnetic moments of electrons (spin and orbit) and nuclei (spin) on an atomic or molecular level. Such effects lead to spectroscopic level shifts that can be detected in optical transitions (Zeeman spectroscopy, MCD spectroscopy, ODMR spectroscopy) or they become the basis of genuine magnetic spectroscopy (ESR and NMR) which have had a huge impact on the development of chemistry since they represent powerful methods of structural analysis. While these spectroscopic methods may be characterized as tools of structural and dynamic *probing* of chemical systems, the advent of spin chemistry, an area dealing with dynamic effects of unpaired spins, has, in principle, opened up the possibility of magnetic *control* of reaction rates and yields. Until now, however, such effects, too,

[a]The classification by the terms in parentheses has been suggested by Y. Tanimoto.

are usually employed for the *diagnostics* of reaction mechanisms. The understanding and interpretation of effects of the first group typically requires quantum mechanical treatment of spin systems and, eventually, of orbital motions of electrons.

The second group of phenomena is concerned with thermal equilibrium states of macroscopic systems in magnetic fields. In such situations macroscopic samples adopt net magnetizations that are particularly strong and depend on temperature if the molecules or atoms composing the sample have unpaired electron spins. The temperature and magnetic field dependence of the magnetization bears important clues as to the magnetic interaction and the degree of cooperativity within the spin system. Such effects are of great current interest in molecular magnetism, a modern field that has developed from classical magnetochemistry that was traditionally interested in the magnetic properties of individual molecules or metal complexes. For chemical reactions with different magnetic moments of starting and product materials the free energy of reaction depends on the external magnetic field strength. Thus, in principle, chemical equilibrium can be shifted by external magnetic fields and the phenomenon can be treated within the formalism of chemical thermodynamics.

Classical mechanics is the domain of the third group of effects. Magnetic forces tending to orient magnetic dipoles along the magnetic field direction or to move them along the gradient of an inhomogeneous field are usually too weak to affect single molecules of low molecular weight in condensed phases because at normal temperatures the magnetic energy is small as compared to kT. However, for macromolecules, mesoscopic particles, or crystals even if they are diamagnetic, the magnetic energy can be high enough to achieve significant effects of orientational ordering at room temperature. Examples of effects based on the forces in inhomogeneous magnetic fields are gas flow and levitation. Another type of effects that can be assigned to this group is due to the Lorentz force on ions undergoing directed translational motion like in electrolytic currents or in stirred solutions. Magnetohydrodynamic effects that ensue macroscopically from such Lorentz forces can affect the rate of heterogeneous electrochemical reactions like corrosion or electrolysis.

In this chapter we present a selection of examples illustrating the principles and current interest in the three groups of effects. A somewhat broader representation of spin chemistry may be conceded to the authors' interests and research activities in this field. Magnetic resonance aspects will not be considered. All equations involving magnetic quantities and their units will be represented in compliance with the rationalized MKSA system.

2 Zeeman Effects

The Zeeman Hamiltonian of a bound electron in a magnetic field $\mathbf{B_0}$ is

$$H_Z = \beta \left(\mathbf{L} + g_e \mathbf{S} \right) \mathbf{B_0} \tag{1}$$

where β is Bohr's magneton, $\mathbf{L}$ the operator of angular momentum, $\mathbf{S}$ the spin operator of the electron, and g_e the g-factor of the free electron. Normally, the Zeeman effect refers to level splittings of magnetic multipletts caused by a magnetic field $\mathbf{B_0}$. Due to its typical size ($1\ \mathrm{cm}^{-1}$ in a field of 1 T) it is directly observable in spectra only if the line width is small enough; this is typically the case only for optical spectra of atoms, ions or small molecules

in the gas phase or for the zero-phonon lines of chromophores in crystalline solids at low temperature [1]. In the following sections dealing with magnetic circular dichroism (MCD), magnetic fluorescence quenching, and spin chemistry we shall understand "Zeeman effects" in a broader sense, namely as comprising all electronic effects that are due to the operator represented in equation (1).

2.1 Magnetic Circular Dichroism

In molecular electron absorption spectroscopy, transitions usually appear as broad bands due to the combination of electronic and vibrational transitions. Thus, energetic shifts on the order of 1 cm^{-1} due to the Zeeman effect in fields of some tesla usually cannot be resolved. Nevertheless, Zeeman effects give rise to the appearance of significant linear and circular dichroisms, of which magnetic circular dichroism (MCD) is the most important. For reviews on the theory of MCD cf. references 2 and 3. Three different contributions, traditionally designed as the A, B, and C terms, add to $\delta\epsilon$ the difference between the absorption coefficients ϵ_{lcp} and ϵ_{rcp} of left and right circularly polarized light:

$$\frac{\delta\epsilon}{E} \propto \left[\left(-\frac{\partial f(E)}{\partial E}\right) A + \left(B + \frac{C}{kT}\right) f(E)\right] \ . \tag{2}$$

Here E is the energy of the absorbed photon and $f(E)$ the line shape of the transition. The A term arises in case of a magnetic splitting of the final level of a transition and its spectral shape corresponds to the first derivative of the underlying absorption band. The B term arises from the Zeeman mixing of levels involved in the optical transition with other electronic levels that are energetically close but not directly involved in the transition. According to first order perturbation theory this term is proportional to the inverse of the energy separation between the coupling levels. The B term gives the dominant contribution to MCD in the case of aromatic organic molecules [4]. The C-term arises in case of degenerate ground states. Absorption transitions from the different Zeeman levels of the ground state do have different circular polarization. In zero field and in low fields the different polarizations of all the Zeeman components cancel. However, if the Zeeman splitting becomes significant in comparison to kT, the difference in Boltzmann populations will lead to a net MCD which increases with decreasing temperature. Of course, the Curie-type dependence indicated in equation (2) is only valid for $\beta B_0 \ll 2kT$. For $\beta B_0/2kT \gg 1$ the temperature dependence approaches a saturation limit. The C term is particularly important for paramagnetic transition metal complexes near liquid helium temperature where it dominates the MCD spectra.

MCD has become an important spectroscopic technique for the structural characterization of transition metal complexes particularly in the area of bioinorganic chemistry with its main focus on the active metal centers in metalloenzymes [5]. In its potential to characterize the magnetic properties of the ground state of such complexes, MCD is comparable to EPR but it also has some complementary potential [6]. For example it has a wider scope of assessing zero-field splittings and it permits investigation of even-electron (non-Kramers) systems that are usually difficult to study with EPR. Furthermore, exchange interactions between interacting magnetic centers can be assessed in a wider range.

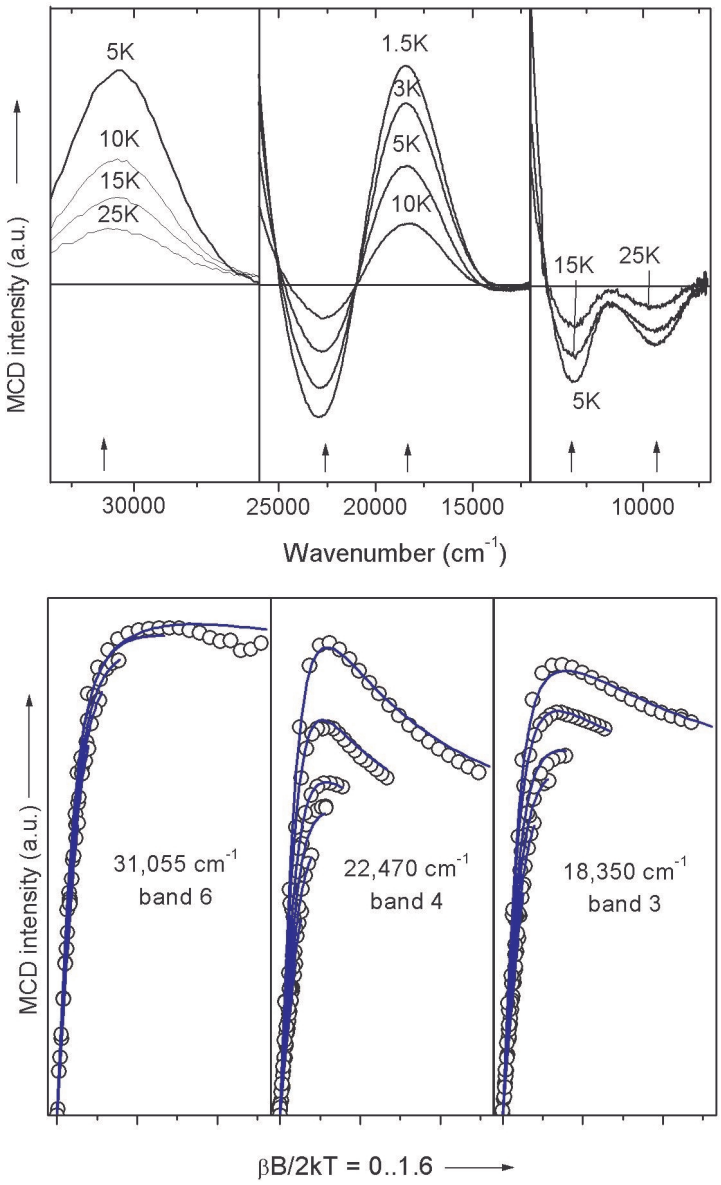

Figure 1: MCD Data for the complex $[Fe(EDTA)(O_2)]^{3-}$. Upper part: Variable temperature MCD data in the near UV, visible, and near-infrared regions. Lower part: Variable temperature/variable Field data recorded at the positions marked by arrows in the upper panel. Open circles - experimental data. Full lines - theoretical fits. Reprinted from reference 7 with permission; copyright 1999 The American Chemical Society.

The example in Figure 1 may be used as an illustration of the information content of variable temperature, variable field (VTVH) MCD-spectroscopy [7]. The complex $[Fe(EDTA)(O_2)]^{3-}$ is a high spin ($S = 5/2$) Fe(III) complex. It shows a variety of peroxo to iron LMCT transitions in the near UV and visible regions that are readily resolved with MCD spectroscopy (Figure 1, upper panel) where the absorption spectra only display broad, unstructured bands. For such complexes the MCD spectra are dominated by temperature dependent C-terms. Furthermore, at high magnetic fields of several tesla and liquid helium temperatures the C-term intensity no longer varies linearly with $1/kT$. Under these circumstances, the temperature and field dependence of the MCD for each individual band (expressed as a function of the dimensionless parameter $\beta B/2kT$) provides two basic pieces of information: (a) information about the linear polarization of the band under investigation although the data are taken on *randomly oriented molecules* in frozen solution and (b) information about the magnetic properties of the *ground state*, i.e. the zero field splitting parameters D and E/D. Thus, a careful VTVH-MCD study simultaneously provides a wealth of information about the ground *and* the various excited states of the compound under investigation that might not be readily accessible with other techniques. Especially when combined with complementary methods such as resonance Raman spectroscopy, MCD gives considerable insight into molecular electronic structure.

2.2 Magnetic Fluorescence Quenching in the Gas Phase

The first case of magnetic quenching of luminescence was reported for iodine vapor by Steubing [8] in 1913 and later interpreted by van Vleck [9] as being due to magnetically induced predissociation. However, a systematic investigation of magnetic fluorescence quenching of molecules in the gas phase was not begun before the seventies when such experiments were undertaken to achieve a better understanding of the radiationless deactivation of electronically excited states in molecules. Since then magnetic quenching of gas phase fluorescence has been described for many molecules from small inorganic ones such as NO, NO_2, CS_2, and SO_2 to larger organic ones such as glyoxal, biacetyl and pyrimidine. Japanese groups have been particularly active in this field. For reviews see references 10–12.

The various types of magnetic field dependences found for magnetic fluorescence quenching of molecules in the gas phase can be assigned to two characteristic mechanisms: the "direct mechanism" or the "indirect mechanism" or combinations of both of these [10,12]. The direct mechanism for which the term $\mathbf{LB_0}$ in the Zeeman Hamiltonian is responsible, is due to the coupling of the fluorescent singlet state (S_i) to a rotational-vibrational manifold of a lower singlet. If the final state manifold is sufficiently dense, the rate constant of non-radiative decay of S_i is given by the golden rule expression

$$k_{nr} = \frac{2\pi}{\hbar}|V|^2\rho \tag{3}$$

where V is the coupling matrix element between the initial and final electronic states and ρ the density of states in the final state manifold that is isoenergetic with the initial state. Since in the direct mechanism $V \propto B_0$, the field dependence of the fluorescence decay rate

constant k is of the form

$$k = k_0 + \alpha {B_0}^2 \tag{4}$$

where α is a proportionality constant. As the fluorescence intensity S is proportional to k_f/k, where k_f is the rate constant of fluorescence emission, the following relation should hold:

$$\frac{\alpha {B_0}^2}{k_0} = \frac{S(0)}{S(B_0)} - 1 \ . \tag{5}$$

Thus, plotting the function $S(0)/S(B_0) - 1$ versus ${B_0}^2$ should give a straight line for the direct mechanism.

In the indirect mechanism, the fluorescent singlet decays radiationless via spin-orbit coupling through an intermediate triplet state. Here the role of the magnetic field is only to modify, through the term $\mathbf{SB_0}$, the energy eigenstates within the triplet manifold but not the coupling between photoexcited state S_i and intermediate T, nor between T and the final ground state manifold. Thus, the operator $\mathbf{SB_0}$ does not enter into the matrix element of the golden rule expression. It was an important discovery that, in case of the indirect mechanism, the fluorescence is basically bi-exponential[15]. This occurs only if the number of ro-vibronic levels in the T-manifold that couple to the fluorescent state S_i is small. Then the initial fast part of the decay can be, qualitatively, interpreted as the establishment of a kind of statistical mixture between the initially excited singlet level and a nearly isoenergetic section of the sparse triplet manifold, while the slow part of the decay is determined by the irreversible decay of the triplet. An external magnetic field increases the amplitude of the fast decay component and decreases that of the slow one which is explained as follows. In zero field the eigenstates in the triplet manifold are spin quantized in the molecular frame and molecular symmetry prohibits spin-orbit coupling between the initial singlet and some of the triplet components. In an external magnetic field the spin is requantized in the laboratory frame and now the initial singlet is spin-orbit coupled to all triplet substates. Thus, in the T-manifold the number of ro-vibronic levels coupled to S_i is increased by up to a factor of 3, meaning that the initial fast decay component adopts a larger amplitude since S_i can be "diluted" with more of the intermediate triplet-levels. As a result, the integral fluorescence intensity decreases. According to these principles the indirect mechanism of fluorescence quenching has to exhibit a saturation behavior with the saturation limit being approached when B_0 exceeds the zero field splitting of the triplet sublevels.

Application of high magnetic fields is of interest when indirect and direct mechanisms of fluorescence quenching are to be separated. As an example we show the results of experiments by Hayashi et al.[16] where fairly high magnetic fields of several tesla have been applied (cf. Figure 2). As is borne out in the Figure, the magnetic fluorescence quenching of SO_2 is saturated at fields below 2 T meaning that this case is controlled by the indirect mechanism, whereas no saturation is obtained up to 6 T for the fluorescence of CS_2 from some vibrationally selected excited singlet states. In the latter case at high fields the magnetic field dependence seems to turn to a ${B_0}^2$-dependence that is characteristic for the direct mechanism.

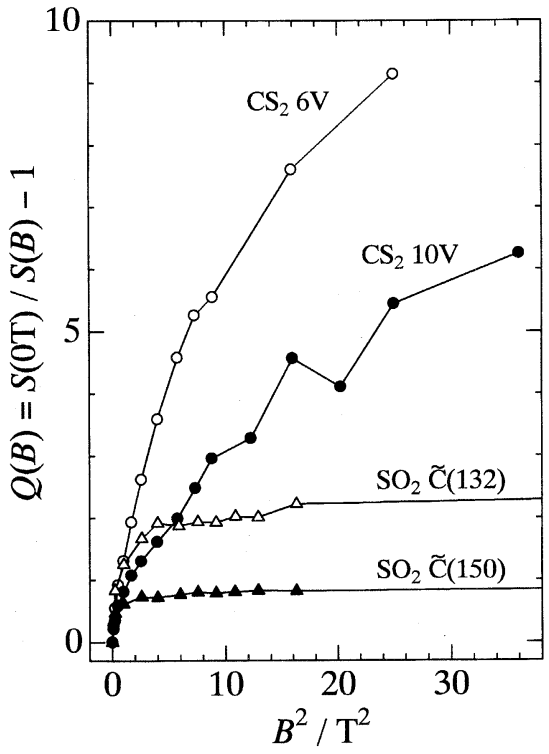

Figure 2: Magnetic field dependence of magnetic quenching observed at room temperature for CS_2 and SO_2 photoexcited into selected vibronic levels. Reprinted from reference 13 with permission; copyright 1998 Kodansha Ltd.

2.3 Spin Chemistry

Spin chemistry has been established as a new field of research since the late sixties (for reviews see references 10, 12, 17, 18). It is essentially concerned with the interplay between spins and chemical kinetics. Basically there are two kinds of effects that follow from such an interplay. First, in an external magnetic field chemical products may be formed with non-Boltzmann distribution of magnetic spin states. This is the area of chemically induced magnetic polarization, known as CIDEP for electron spins and CIDNP for nuclear spins. Second, external magnetic fields can modify chemical yields and chemical kinetics if reaction intermediates with unpaired spins are involved. In the following we will deal with this second kind of effect.

The central mechanism of spin chemistry is the radical pair mechanism (RPM) with its paradigm of spin conservation during chemical reaction steps creating or eliminating radical pairs (RPs). Typical chemical reactions generating RPs are electron or hydrogen atom transfer reactions and homolytic bond cleavage. RPs may decay chemically by pairing the radical electrons in electron or hydrogen atom transfer reactions or in covalent bond formation, or physically by diffusive separation into free, uncorrelated radicals in the bulk.

A general scenario for the RPM based on electron transfer processes is shown in Figure 3. Usually, photoexcitation is necessary to affect electron transfer between two closed-

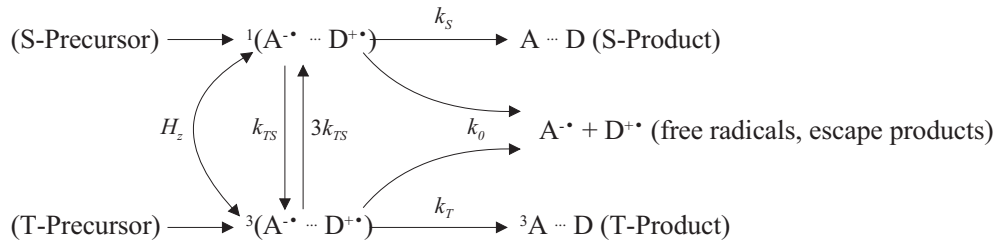

Figure 3: General scenario for the radical pair mechanism based on electron transfer processes.

shell reactants. Depending on whether the photoreaction starts from an excited singlet or triplet state, the RP originates with singlet or triplet multiplicity where the two unpaired electron spins are in an anti-parallel or parallel alignment, respectively. Following the spin conservation rule, only singlet product formation is allowed for singlet radical pairs and triplet product formation for triplet pairs. Of course, further restrictions are due to the thermodynamics of the reaction considered. Thus, electron backward transfer in the RP to generate the singlet ground state of the reactants is usually associated with a large drop in free energy, while formation of a locally excited triplet state is possible only for very energy-rich RPs. Diffusive separation of chemically unlinked RPs to free radicals in the bulk is allowed both from the spin as well as the energetic point of view and thus represents a reaction channel equally open for singlet and triplet RPs.

The spin selectivity of the reactions of the RP renders the RP decay and the yields into the different product channels sensitive to the T/S ratio. As singlet and triplet RP states are energetically almost degenerate, (see below) changing this ratio requires only a small (i.e. smaller than kT) if any energy exchange with the lattice. These interactions can be described by an effective spin Hamiltonian comprising the following parts:

$$H_{spin} = H_Z + H_{ex} + H_{hfc} + H_{dip} + H_{sr} \ . \tag{6}$$

Here the Zeeman Hamiltonian is represented as

$$H_Z = \beta \left(\mathbf{S_1 g_1} + \mathbf{S_2 g_2} \right) \mathbf{B_0} \tag{7}$$

where $\mathbf{S_1}$ and $\mathbf{S_2}$ denote the spin operators of the two radicals and $\mathbf{g_1}$ and $\mathbf{g_2}$ are the g-tensors of the two radicals. Note that in this representation the magnetic contribution of orbital angular momentum is projected into an effective spin whereby the electronic g-factor is changed to a g-tensor with characteristic values depending on the electronic structure of the radical. In high magnetic fields, the Zeeman part of the spin Hamiltonian will dominate the spin behavior (cf. Figure 4). Therefore, we will discuss the other parts only qualitatively. The exchange interaction (H_{ex}) causes an energetic splitting of singlet and triplet; this falls off approximately exponentially with the distance between the two unpaired spins. Around 10 Å the exchange interaction has approximately come down to some 10 G, the typical order

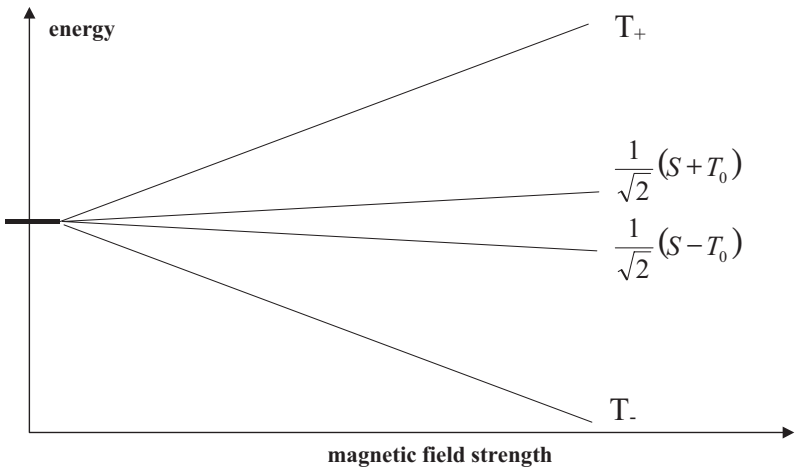

Figure 4: Magnetic field dependence of energy eigenvalues for the Zeeman Hamiltonian given in equation (7).

of magnitude of the hyperfine interaction, represented by the third, distance-independent term (H_{hfc}) in equation (6). The magnetic dipolar interaction (H_{dip}) between the two unpaired electron spins decays with the cube of the distance. Around 10 Å it is typically of the same order as the hyperfine interaction. Spin-rotational interaction (H_{sr}) usually is still smaller than the two former interactions.

If we neglect all parts of the spin Hamiltonian that are small relative to H_Z, the scheme of energy eigenvalues is as shown in Figure 4. While the triplet components T_+ and T_- correspond to the highest and lowest eigenstates, respectively, the central eigenstates are mixtures of T_0 and S and their energy splitting increases with the magnetic field as $\beta\Delta g B_0$ where Δg is the difference of the actual g-values of the two radicals for a specified orientation (if the rotational frequency is small in comparison to $\beta\Delta g B_0/\hbar$) or the differences of the isotropic averages of the two g-factors (if the rotational frequency is large in comparison to $\beta\Delta g B_0/\hbar$). It is important for the understanding of RP spin dynamics that neither T_0 nor S are stationary spin states for the situation represented in Figure 4, but that once generated in a chemical process they are coherently converted into each other with an angular frequency of $\beta\Delta g B_0/\hbar$ corresponding to the difference of the Larmor frequencies of the two unpaired electron spins. Actually this motion establishes a kind of internal clock in the system that is externally tunable with the magnetic field strength B_0. This magnetic clock can be used to measure the chemical rate processes in the reaction scheme. The way to "read" this clock is to observe the magnetic field dependence of the final product yields. Thus, the actual reading process can be much slower than the real processes that determine the magnetic field dependence.

For a complete description of the spin conversion kinetics in the RP, the role of incoherent relaxation processes has to be included. These processes arise from the effect of fluctuating parts of the spin Hamiltonian (g-tensor and hyperfine coupling anisotropy, electron spin-spin dipolar interaction, spin rotational coupling) [19] but may be also due to

Orbach processes involving thermal excitation of higher electron levels of the radicals [20]. Phenomenologically, the relaxation kinetics can be described by the rate constants k_{TS} and $k_{ST} = 3\ k_{TS}$, their ratio assuring establishment of the correct spin statistical equilibrium. In interpreting the magnetic field effect on the overall kinetics, attention has to be paid not only to the field dependence of the coherent singlet-triplet mixing processes but also to the field dependence of the relaxation processes if they give a kinetically significant contribution[21,22]. In the following we present a few examples representative of high magnetic field applications in spin chemistry.

The primary processes of photosynthesis have attracted the attention of spin chemists at an early stage [23]. Here the photoexcited singlet state of a special pair (P) of chlorophyll molecules in the photosynthetic reaction center transfers an electron to a primary acceptor (Φ), a pheophytin molecule in case of plant photosystem II or bacterial reaction centers. Thus, the primary RP ($P^{+\bullet} \cdots \Phi^{-\bullet}$) originates with singlet spin. In the natural systems, the electron is then transferred further to a quinone Q and does not return to $P^{+\bullet}$. However, in preparations where the quinone is pre-reduced or removed, the primary RP decays solely by recombination which on energetic criteria can yield both the singlet ground state product ($P \cdots \Phi$) and the excited triplet product ($^3P \cdots \Phi$). Of course, the second channel is only open after a $^1(P^{+\bullet} \cdots \Phi^{-\bullet})$ to $^3(P^{+\bullet} \cdots \Phi^{-\bullet})$ spin conversion process has occurred. In zero field this process is efficiently induced by the hyperfine coupling in the two radicals such that sizeable triplet yields ensue. In low magnetic fields the triplet yield decreases since the hyperfine coupling between S and $T_\pm$ is rendered ineffective once the Zeeman splitting exceeds the hyperfine interaction which is of the order of several 10 G. At high fields the Zeeman-type S/T_0 mixing becomes effective: for a Δg of 0.001 the $\beta \Delta g B_0$ term amounts to 10 G in a field of 1 T. As observed by Boxer et al.[24,25,26] the increased $S \rightarrow T_0$ rate gives rise to an increasing triplet yield at high field. At 5 T, the highest field employed in this work, this even exceeds the triplet yield in zero field, thus making fully up for the field induced suppression of hyerfine-induced $S/T_\pm$ mixing at low fields.

In photosynthetic reaction centers the reacting components have little mobility towards each other since they are firmly held in position by the interaction with a protein matrix. This situation is rather characteristic of a solid state reaction system. In liquid solutions RPs will dissociate rapidly, in particular if no attractive Coulomb forces are active between them. Thus, in liquid solution this non-spin-selective reaction channel will always play a dominant role. In order to make the Zeeman type S/T_0 process fast enough to be competitive, the Δg value should be high. In organic systems this can be achieved if electron spin density is localized on heavy heteroatoms. A recent example of an investigation in high magnetic fields of such a system has been reported by Wakasa et al.[27] They studied the H-atom transfer reaction

$$^3\mathrm{MBP} + \mathrm{PhSH} \longrightarrow {}^3(\mathrm{MBPH}^\bullet \cdots \mathrm{PhS}^\bullet) \longrightarrow \mathrm{MBPH}^\bullet + \mathrm{PhS}^\bullet \qquad (8)$$

between triplet excited 4-methoxybenzophenone (MBP) and thiophenol (PhSH) detecting the yield of formation of free radicals by laser flash spectroscopy (cf. Figure 5).

In this system the primary RP originates with triplet spin. Recombination to an excited triplet product is excluded due to energetic reasons. RP recombination to the starting

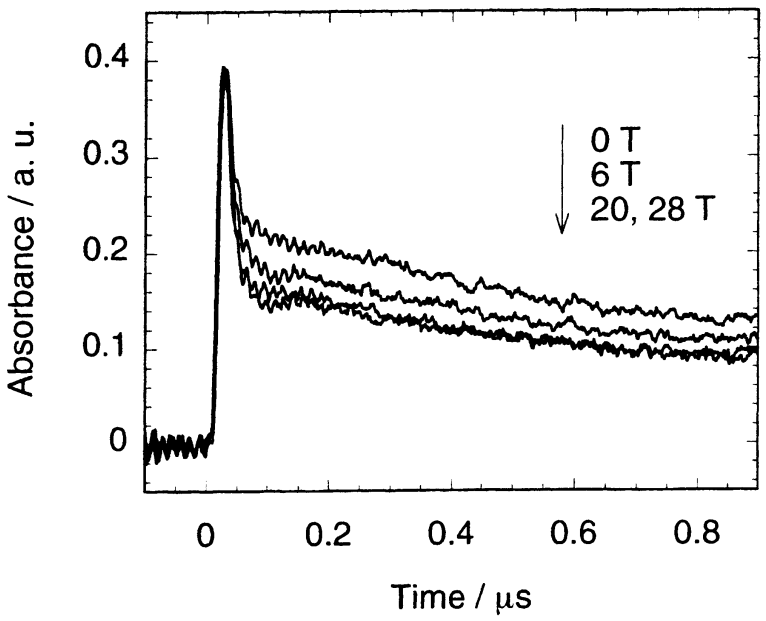

Figure 5: Transient absorption curves observed for the hydrogen abstraction of triplet 4-methoxybenzophenone from thiophenol in 2-methyl-1-propanol at 0, 6, 20 and 28 T. The fast initial decay monitors the decay of the triplet, the long lived component is due to free radicals originating in the triplet quenching process. Reprinted from reference 27 with kind permission of H. Hayashi; copyright 1999 The American Chemical Society.

compounds in their singlet ground states requires a $T \rightarrow S$ process to occur before the RP dissociates. In the RP ($MBPH^{\bullet} \cdots PhS^{\bullet}$), Δg amounts to 0.0055. Thus, at 1 T a value of 55 G for $\Delta g B_0$ is reached, corresponding to a T_0/S conversion time of about 1 ns which leads to a sizeable recombination of the RPs before dissociation. This gives rise to the remarkably strong magnetic field effect shown in Figure 6. Applying the field from a pulsed magnet with a pulse duration of $\sim$ 1 ms the effect has been observed up to 28 T. For this field the value of $\Delta g B_0$ is 1540 G which corresponds to a T_0/S conversion time of about 35 ps. This time seems short enough to allow recombination of all RPs created in T_0 . Consequently, as $\sim 1/3$ of all RPs are generated in the T_0 state, a maximum decrease of the radical yield of $\sim$ 30 % is observed in the saturation limit.

A quantitative simulation of the field dependence has been performed on the basis of a model according to Freed [28] and Pedersen [29] that accounts for Δg-type T_0/S mixing and treats the separation of the radicals by a continuous diffusion equation. The experimental results can be reasonably fitted (cf. Figure 6) if the initial T_0 population of the RP is corrected for some magnetic field dependence of the initial T_0 population that is due to the triplet mechanism [30].

In the RP system investigated by Wakasa et al. the Δg of 0.0055 corresponds to a magnetic clock with a period of $\tau_L \approx 1$ ns at 1 T. We note here that in this work the rate process actually probed by the magnetic clock is the dissociation of the RP. An effective rate

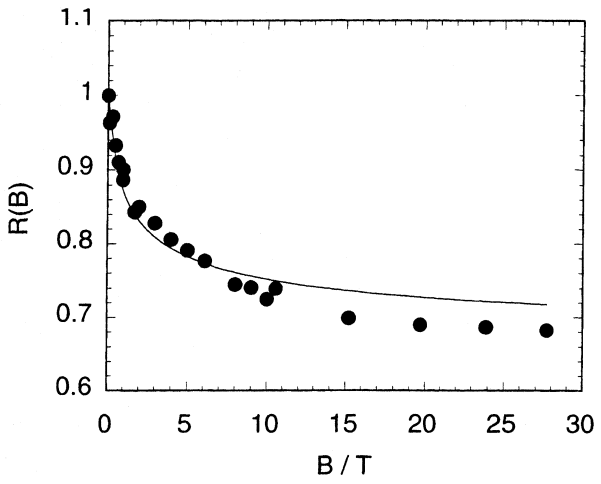

Figure 6: Relative change of free radical yield in the ^{3}MBP$\cdots$PhSH system as a function of magnetic field. The solid line represents a best fit according to the model indicated in the text. Reprinted from reference 27 with kind permission of H. Hayashi; copyright 1999 The American Chemical Society.

constant of dissociation k_0 can be estimated by the Eigen-Debye relation in combination with the Stokes-Einstein relation

$$k_0 = \frac{3D}{d^2} \approx \frac{2kT}{\pi d^3 \eta} \tag{9}$$

where d is the RP recombination distance, D the sum of the diffusion coefficients of the two radicals and η the solvent viscosity. Using the parameter values given in reference 27 (d = 5 Å, $\eta = 3.33$ cP), a value of 6.3×10^9 s^{-1} is obtained for k_0. For $\Delta g = 0.0055$ the magnetic field that would produce an equivalent clock time of k_0^{-1} is 6.5 T which in fact corresponds to a field where the magnetic field effect curve enters the saturation zone.

For RP systems where Δg is of the order of unity one would have $\tau_l \approx 5$ ps at a field of 1 T, such that much shorter rate processes could be measured through magnetic field effects on product yields. RPs with such properties can be realized if paramagnetic metal complexes with an unpaired electron in nearly degenerate d-orbitals are involved. For such species a very strong orbital contribution arises leading to g-tensor values strongly deviating from that of the spin-only value, such that for RPs composed of these paramagnetic metal complexes and normal organic radicals Δg can indeed reach values around unity. The following spin-chemical examples will deal with RPs involving Ru(III) and Fe(III) complexes with low spin d^5 electron configurations and $S = 1/2$ ground states, such that their spin chemistry can be described in the framework of the RP mechanism.

Photoelectron transfer reactions between Ru(II)-trisbipyridine ($Ru(bpy)_3^{2+}$) or related complexes and methylviologen (MV^{2+}) (for structures see Figure 7) have served as kind of standard reaction for many studies interested in principal aspects of the outer sphere electron transfer mechanism [31]. After photoexcitation and rapid intersystem crossing the

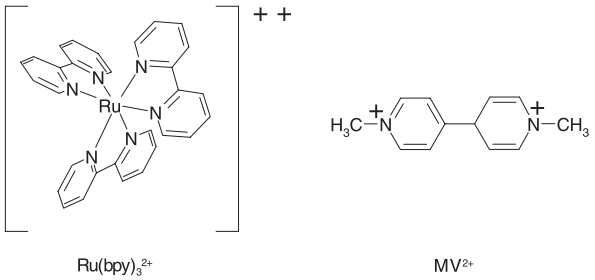

Figure 7: Structures of Ru(II)-trisbipyridine ($Ru(bpy)_3^{2+}$) and methylviologen (MV^{2+})

Ru-complex in its excited triplet state transfers an electron to methylviologen, a very good organic electron acceptor. Hence the RP ($Ru(bpy)_3^{3+} \cdots MV^{+\bullet}$) is formed with triplet

$$^3Ru(bpy)_3^{2+} + MV^{2+} \longrightarrow^3 \left(Ru(bpy)_3^{3+} \cdots MV^{+\bullet}\right) \longrightarrow Ru(bpy)_3^{3+} + MV^{+\bullet} \qquad (10)$$

spin. For energetic reasons, formation of triplet products is not possible. Only the recombination, i.e. backward electron transfer, regenerating the initial reactants in their singlet ground states is feasible. Thus, we are dealing with the analogous spin chemical situation as in the previous example. In the present system, however, even in zero field the quantum yield of free radicals is only of the order of 20 % implying that an efficient mechanism for spin relaxation exists in the RP. This is in accordance with the fact that Ru(III) complexes have very short spin relaxation times [20]. Nevertheless a full S/T equilibrium is not established during the life time of the RP and the coherent magnetic acceleration of the T/S process has still kinetic consequences on the yield of free radicals. As shown in Figure 8 the field dependence of this quantity has been measured for several Ru-complexes with either bipyridine or phenanthroline ligands or a mixed sphere of the two types of ligands [32]. In order to vary the field up to 17 T, a Bitter type magnet at the High Magnetic Field Laboratory of CNRS/MPG at Grenoble was used. The free radical yield was measured under continuous illumination conditions exploiting the fact that the $MV^{+\bullet}$ radicals become very long lived if the free Ru(III) complexes are scavenged by "sacrificial" electron donors.

Application of a magnetic field decreases the free radical yield in the system as should be expected from the fact that a magnetic acceleration of the T/S process favors RP recombination which here is only possible in the singlet channel. The magnetic field effects for the four complexes differ in their amplitudes indicating a systematic structural dependence of the magnetic field effect. The effects saturate above about 10 T and the half field value is about 3 T, corresponding to a T/S mixing time of about 5 ps from which we can qualitatively tell the time scale underlying all the processes by which the photo-generated RPs decay. A quantitative analysis of the field dependence has been performed in order to determine the values of the characteristic kinetic parameters k_{TS} , k_S and k_0 (for their definition cf. Figure 3, the numerical values are given in Table 1). This analysis is based on the numerical solution of a stochastic Liouville equation for the spin density matrix of the RP. In particular, the anisotropy of the Zeeman Hamiltonian and magnetic field independent

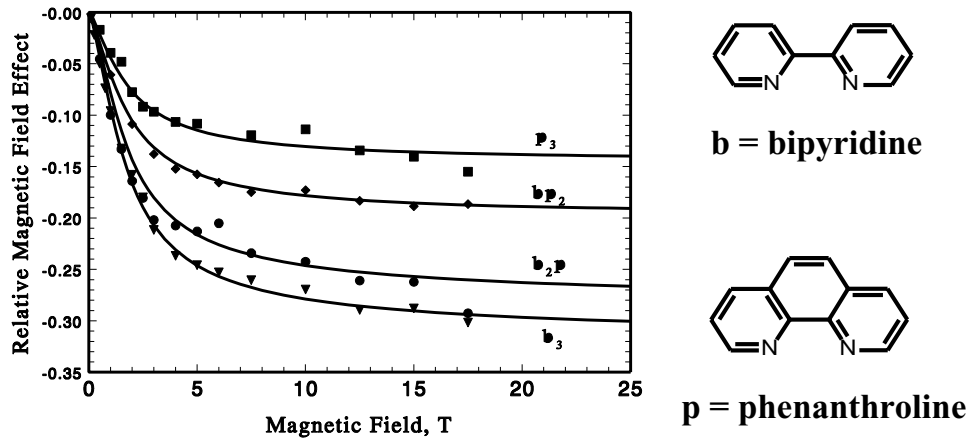

Figure 8: Relative magnetic field effect on the quantum yield of $MV^{+\bullet}$ radical production in the photoreaction with various Ru(II)-tris-diimine complexes (b = bipyridine, p = phenanthroline). The curves are results of theoretical simulations using the parameters given in Table 1. Reprinted from reference 32; copyright 1993 Verlag Chemie.

(Orbach type) spin relaxation is explicitly taken into account. In order to properly account for the singlet spin selectivity of RP recombination, the spin-orbit-coupling induced contamination of the RP triplet with higher singlets and of the RP singlet with higher triplets is explicitly considered. The degree of contamination can be calculated using the experimental g-tensor values. The rate constants of dissociation of the RPs correspond to

Table 1: Characteristic reaction parameters for the decay of the RP ($RuL_3^{3+} \cdots MV^{+}$)

Ligands	Parameters		
	k_0 [10^9 s^{-1}]	k_S [10^9 s^{-1}]	τ_s^* [ps]
b_3	2.3	78	27
b_2p	2.2	66	24
bp_2	1.9	46	21
p_3	1.5	32	19

* τ_s is related to k_{TS} in Figure 3 by $\tau_s = \frac{1}{(4k_{TS})}$

dissociation life times of about 0.5 ns which is even somewhat slower than the corresponding parameters in the purely organic RP ($MBPH^{\bullet} \cdots PhS^{\bullet}$). However, the time constants τ_s of RP spin relaxation (corresponding to the spin relaxation time of the Ru(III) complex, because spin relaxation in the $MV^{\bullet+}$ radical is much slower) are all found around 20 ps which, in combination with the high rate constants of backward electron transfer in the singlet channel (k_S), places the RP decay on a time scale 100 times shorter than in case of the organic RP ($MBPH^{\bullet} \cdots PhS^{\bullet}$). Thus, even though the Δg factor is approximately 100 times larger, the field necessary to make the value of $\beta \Delta g B_0/\hbar$ match the intrinsic kinetic

time scale is very similar to that of the organic RP. Hence, in spite of the large difference in the RP decay kinetics, the observed magnetic field dependencies for the two systems are very similar (note the onset of saturation around 5 T for the Ru-curves).

The structural influence that is reflected in the results of the four complexes can be related to two factors. First, the larger size of the phenathroline ligand leads to a larger distance of closest approach of the centers of the two reactants. This will qualitatively explain the decrease of k_0 with increasing number of phenanthroline ligands (cf. equation (9)) and of k_s (the rate constant of electron transfer falls off exponentially with distance). Second, the energy of the lowest excited state of the Ru(III) complex decreases for each bipyridine ligand that is replaced by a phenanthroline ligand. Since it is this excited state via which the Orbach type spin relaxation occurs, a lowering of this state reduces the activation barrier of the process and therefore accelerates spin relaxation. The energy of the lowest excited state has been derived from temperature dependent measurement of τ_s for the Ru(III) complexes by NMR. The pertinent results have independently confirmed not only the relative order of the τ_s values of the four complexes obtained by the magnetic field effect but also their absolute size [33].

In the two previous examples the magnetic Larmor clock has been "read" by determining free radical yields on a time-scale much longer than the actual period of the clock. Recently, the present authors and collaborators reported on sub-picosecond time-resolved experiments with a real-time chemical monitoring of the magnetic Larmor clock [34]. Here a photoexcited dye (oxonine, Ox^+) reacts with the electron donor ethylferrocene (Fc-Et) according to

$$^1\left(Ox^+\right)^* \cdots Fc-Et \longrightarrow ^1\left(Ox^\bullet \cdots Fc-Et^{+\bullet}\right) \longrightarrow Ox^+ \cdots Fc-Et\ . \qquad (11)$$

This is present in very high concentrations such that on photo-excitation each oxonine molecule is in immediate contact with an electron donor molecule and the rate of forward electron transfer is not limited by diffusion. Actually in this system RPs are formed within 200 fs. Since they originate from singlet excited precursors they are created with singlet multiplicity and the backward electron transfer regenerating the reactants in their singlet ground states is both spin allowed and favorable by the driving force ΔG.

The RP recombination kinetics is recorded using the pump-probe technique with laser pulses of 100 fs width. The signals shown in Figure 9 are observed at a probe wavelength where the depletion and recovery of the oxonine ground state is monitored. As can be seen in the Figure, this recovery is divided into two stages, a fast one with a time constant of about 1 ps and a slower tail extending from picoseconds to nanoseconds.

In the presence of a magnetic field, the fast stage of recombination is not altered but the onset of the slow stage of recombination is shifted to shorter times with higher magnetic field. This effect is due to the coherent S/T mixing process driven by the Zeeman term. Since, as a consequence of the strong spin-orbit coupling at the Fe center, the g-tensor components of the $Fc-Et^{+\bullet}$ species range between 1.3 ($g_\perp$) and 4.4 ($g_\parallel$) and $g(Ox^\bullet) \approx 2.0$, the $\Delta g B_0$ term adopts the same order of magnitude as $g_e B_0$ characterizing the absolute Larmor precession frequency of the free electron spin. The coherence of the magnetic-field induced $S \leftrightarrow T$ mixing is borne out by the fact that at longer times the curves at higher fields curves cross the curves at lower fields meaning that, because of the higher S-character

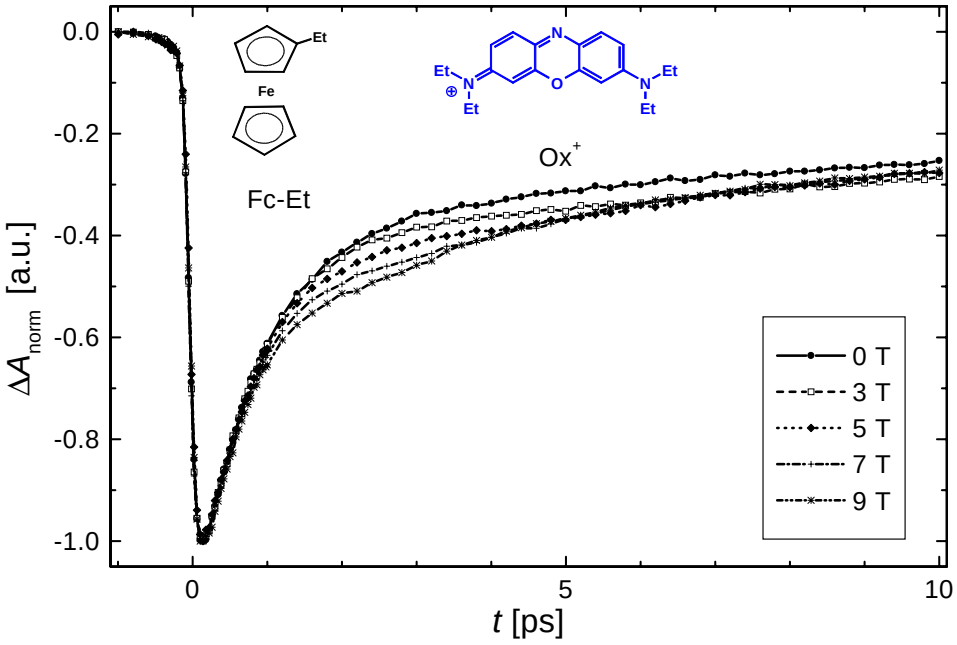

Figure 9: Transient absorption signal of the recombination of the RP ($Ox^{\bullet} \cdots Fc - Et^{+\bullet}$) in acetonitrile. The RP is generated by photoexciting the dye Ox^{+} at 650 nm to its S_1 state. In the presence of high Fc-Et concentrations (2 M) this state is quenched via electron transfer in about 200 fs. The recombination is monitored by the recovery of the ground state of Ox^{+} at 610 nm with laser pulses of 100 fs length. The experiment was conducted in fields ranging from 0 to 9 Tesla at room temperature. Reprinted from reference 34; copyright 1998 American Association for the Advancement of Science.

of the RP after coherent return from T to S, the recombination becomes faster again. The details of the magnetic field effect have been theoretically simulated in a quantitative fashion as is shown in Figure 10 where the differences between in-field signal and zero-field signal are plotted. The pertinent calculation based on a time-dependent solution of the stochastic Liouville equation for the reaction employed the rate constants $k_S = 1.3$ ps^{-1} and $k_{TS} = 26$ ps^{-1} (i.e. $\tau_s = 6.5$ ps) as fit parameters. The Zeeman Hamiltonian was parameterized in accordance with experimental g-tensor values from ESR data. Actually the good agreement between theory and experiment would have allowed to determine the g-tensor values correctly from fitting the magnetic field dependent kinetics. These experiments represent the fastest records of spin chemical effects reported so far. This has increased the limits in time-resolution of spin chemistry by 3 orders of magnitude. On the one hand these results demonstrate that it is possible to magnetically modify the effective rate of electron transfer processes on the picosecond time-scale and on the other hand they represent the first determination of a spin relaxation time constant in the picosecond regime by time domain methods. In addition they exhibit the potential to yield the magnetic parameters of short lived radicals on time scales that will never be accessible to EPR techniques.

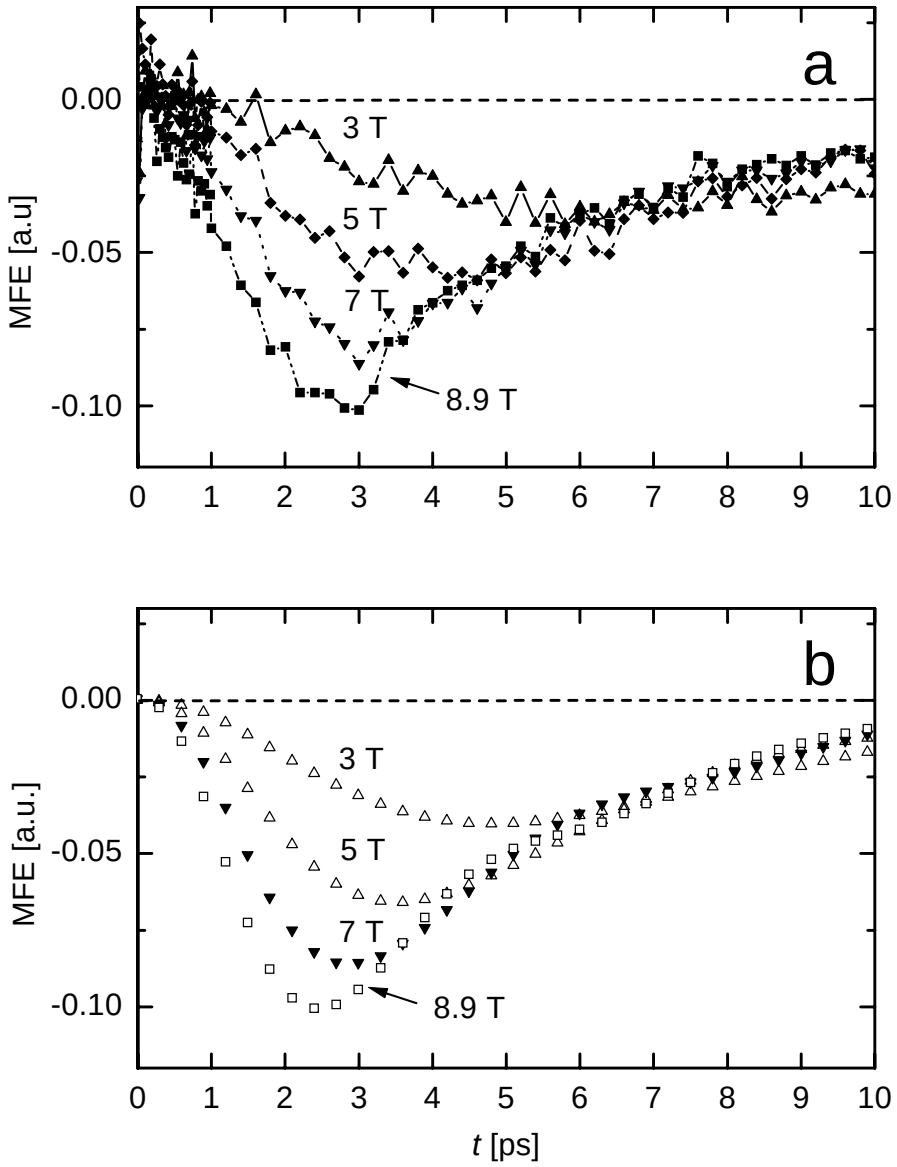

Figure 10: Comparison of experimental and simulated magnetic field effect for the RP ($Ox^{\bullet} \cdots Fc - Et^{+\bullet}$). a) Experimental magnetic field effect defined as the difference of the in-field time traces and the zero-field trace of the data shown in Figure 9. b) Simulations based on the stochastic Liouville formalism. Adapted from reference 34.

3 Thermodynamic Equilibrium

For the thermodynamic equilibrium state of a macroscopic system the magnetic field is just another externally selectable variable of state and all thermodynamic functions will, in general, depend on the value of the magnetic field. Thus, it follows from the magnetic field dependence of the Gibbs free energy G that, in principle, chemical equilibria can be shifted by external magnetic fields. On the other hand, since in a magnetic field each material adopts a certain macroscopic magnetic moment, the magnetization is introduced as a new thermodynamic function. In the following we will review some aspects of these phenomena.

3.1 Chemical Equilibrium

Chemical equilibria are usually characterized by their equilibirum constant K that is related to the standard free energie $\Delta_R G^\ominus$ of the reaction by

$$\ln K = -\frac{\Delta_R G^\ominus}{RT} \ . \tag{12}$$

For a given reaction $\sum \nu_i A_i = 0$ with A_i denoting the reactants ($\nu_i < 0$) and products ($\nu_i > 0$) and the ν_i their stoichometric coefficients, $\Delta_R G^\ominus$ is related to the chemical standard potentials $\mu_i^\ominus$ by

$$\Delta_R G^\ominus = \sum \nu_i \mu_i^\ominus \ . \tag{13}$$

In a magnetic field B_0 (measured outside the sample) the magnetic contribution to $\mu_i^\ominus$ is [35]

$$\mu_{m,i}^\ominus = -\int_0^{B_0} M_i^\ominus dB_0 \ . \tag{14}$$

The molar magnetic moment $M_i^\ominus$ in the standard state of compound i can be written as

$$M_i^\ominus = \chi_i^\ominus \frac{B_0}{\mu_0} \tag{15}$$

where $\chi_i^\ominus$ is the molar magnetic susceptibility in the standard state. For diamagnetic compounds $\chi_i^\ominus$ is independent of the field. The same holds true for paramagnetic compounds as long as $\beta B_0 \ll kT$. For constant $\chi_i^\ominus$ the field dependence of the chemical standard potential is

$$\mu_{m,i}^\ominus = -\frac{\chi_i^\ominus B_0^2}{2\mu_0} \ . \tag{16}$$

Combining equations (12), (13) and (16) the change ΔK of the equilibrium constant of a reaction involving dia- and paramagnetic compounds can be expressed as

$$\frac{\Delta K}{K} = \frac{\Delta_R \chi^\ominus B_0^2}{2\mu_0 RT} \tag{17}$$

where $\Delta_R \chi^\ominus = \sum \nu_i \chi_i^\ominus$. To give an idea of the order of magnitude of the effects to be expected let us assume that $\Delta_R \chi^\ominus = 0.1$ cm^{3}mol^{-1} which is a typical value if, for example,

in the conversion of an $S = 0$ low spin metal complex to an $S = 2$ high spin complex 5 moles of Bohr's magnetons are created. In this case $\Delta K/K$ reaches a value of 1.6×10^{-5} in a field of 1 T at room temperature. This is a pretty small value and requires high precision techniques to be measured. Using optical spectroscopy, effects of this order of magnitude have been detected by Jansen et al.[36] for the complex $(CoL_2)^+$ ($L^- = [C_5H_5Co(POR_2)_3]^-$) dissolved in CH_2Cl_2. For this complex, a diamagnetic low-spin form is in equilibrium with a high-spin ($S = 2$) form. Since the optical absorption spectra of the two forms differ, a shift in the equilibrium concentrations can be observed as a change in optical density. The detected change in optical density follows a B_0^2 dependence. At 23 T, the highest field employed, the extent by which the equilibrium is shifted to the paramagnetic form is about the same as that reached by increasing the temperature by 0.4 K in zero field. Another example reported by this group[36] is the complex $Fe(bt)_2(NCS)_2$ ($bt = 2, 2', -$bisthiazoline) for which the low-spin to high-spin transition was investigated in the solid state by a dilatometric technique. Here the transition temperature for the conversion between the two phases could be shifted by 0.13 K in a field of 10 T, corresponding to a heat of phase transformation of 10 $kJmol^{-1}$ which is in agreement with calorimetric data.

Stronger magnetic effects on chemical equilibria can be expected if ferromagnetic phases are involved. An example for such a reaction is the transformation of ferromagnetic $LaCoH_x$ phases by taking up a further mole of H_2. For example, the transformation of the so-called β-phase ($LaCo_5H_{3.4}$) into the γ-phase ($LaCo_5H_{4.3}$) according to the equation

$$2.22\ LaCo_5H_{3.4}\ (s)\ +\ H_2\ (g) \rightleftharpoons 2.22\ LaCo_5H_{4.3}\ (s) \tag{18}$$

goes along with a change in magnetic moment of $\Delta_R M = 32.8\ JT^{-1}mol^{-1}$. Equilibrium thermodynamics of reaction (18) demands that the hydrogen pressure in equilibrium with a mixture of the β- and the γ-phase should be constant, i.e. independent of the mixing ratio. For ferromagnetic materials where the maximum molar magnetization M_s is reached already in low magnetic fields, equation (16) has to be replaced by

$$\mu_{m,i}^{\ominus} = -M_{s,i}B_0\ . \tag{19}$$

Using this expression, the following thermodynamic relation can be derived

$$\ln \frac{K(B_0)}{K(0)} \equiv \ln \frac{P_{H_2}(B_0)}{P_{H_2}(0)} = \frac{B_0 \Delta_R M_s}{RT}\ . \tag{20}$$

Results of measurements of hydrogen pressure P_{H_2} in equilibrium with mixtures of the β- and γ-phase of $LaCo_5H_x$ obtained by Yamaguchi et al. [14,37] are shown in Figure 11. In a field of 15 T the hydrogen pressure increases by about 20 % which is in excellent agreement with the theoretical result.

3.2 Molecular Magnetism

The focus of traditional magnetochemistry was on the magnetic properties of individual molecules, in particular of paramagnetic metal complexes, as a probe of their electronic

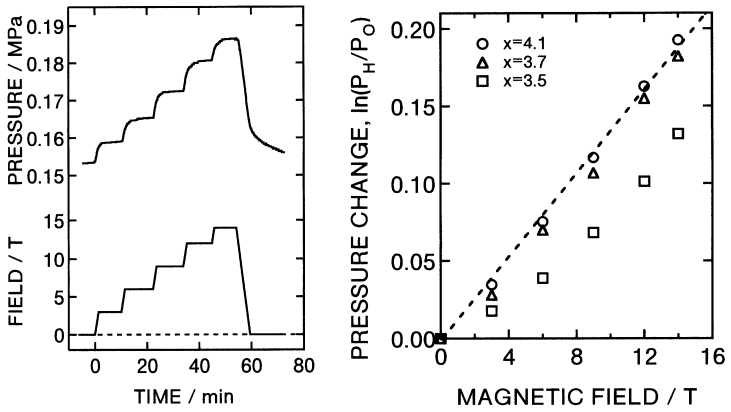

Figure 11: Left: Time variation in hydrogen pressure (upper panel) and magnetic field (lower panel) at 293.2 K for the $\beta - \gamma$ phase equilibrium in the $LaCo_5H_x$ system. Right: Logarithmic pressure change versus magnetic field up to 15 T for the $LaCo_5H_x$ system. The broken line is the theoretical result. For x = 3.5 the deviation of the experimental points from the theoretical line is probably due to the fact that the percentage of the γ-phase present in the reaction system is not yet sufficient to establish full equilibrium during the time of the experiment. Reprinted from reference 14 with permission; copyright 1998 Kodansha Ltd.

structure. The interest of modern magnetochemistry has shifted to supramolecular assemblies and crystals, seeking to understand the chemical basis of magnetic interactions between the magnetic units, i.e. it has moved from simple paramagnetic behavior to collective behavior including many new spin topologies. The search for an understanding of cooperative magnetic properties goes along with the design and synthesis of new materials: molecule-based magnets [38]. The cooperative phenomena of ferromagnetism and ferrimagnetism are only borne out below some critical temperature of the system. An important means to characterize the situation of spin interaction in such systems is to record magnetization curves as functions of magnetic field and temperature. The spin topology of most of the molecule-based magnets is rather complex, so that the effect of a magnetic field is not as straightforward as for classical magnets. In many cases, even at 20 or 30 T, saturation is not reached. This situation is due to the fact that the compounds may present both ferromagnetic and antiferromagnetic interactions between uncompensated spins. It would be beyond the scope of this chapter to go into the theoretical details of intermolecular magnetic interactions. Instead we will present two recent examples of interesting new molecule-based magnetic materials.

The compound $Mn_2(H_2O)_5Mo(CN)_7 \cdot 4.75\ H_2O$ was very recently obtained in large, well shaped single crystals in Kahn's laboratory [39]. It shows ferromagnetic ordering below 51 K and exhibits very interesting anisotropic magnetic behavior. The magnetic Mo^{3+} and Mn^{2+} ions forming a 3-dimensional lattice are connected through CN-bridges. In Figure 12 the field dependence of magnetization along the three magnetic axes is shown. The strong anisotropy is clearly borne out. A "spontaneous" ordering of the spins occurs along the b-axis at fields below 0.12 T. Along the c^*-axis, the magnetization increases most slowly and even at 5 T saturation is not reached. Along a, the magnetization presents an inflection

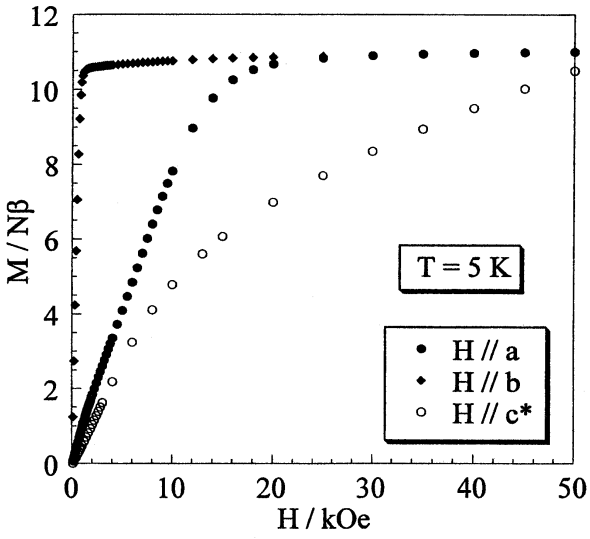

Figure 12: Field dependence of magnetization at 5 K along the three magnetic axes of single crystals of $Mn_2(H_2O)_5Mo(CN)_7 \cdot 4.75\ H_2O$. From reference 39 with permission, copyright 1999 The American Chemical Society.

point around 1 T, and saturation is reached at 2.1 T. This behavior characterizes a field-induced reorientation from the b-direction at low fields to the a direction at high fields. From the temperature and magnetic field dependence of the magnetization along the a-direction a magnetic phase diagram with 5 distinct phases has been derived. For many ferromagnetic compounds the magnetic ordering attained in a magnetic field below the saturation threshold is not a unique function of the field strength but also depends on the history, i.e. on whether the set field values were reached coming from higher or from lower fields. Cycling the field between some high positive and the corresponding negative value will in general produce a magnetization curve characterized as a hysteresis loop. The states on this loop are not thermal equilibrium states but are meta-stable, i.e. they owe their apparent stability to kinetic barriers preventing the establishment of the true and unique equilibrium states. That such barriers exist even in rather interaction-free ensembles of high-spin molcules has been shown for the cluster compound $Mn_{12}O_{12}(CH_3COO)_{16}(H_2O)_4$ (abbreviated as Mn_{12}; for the structure of the cluster see the inset in Figure 13) [40]. In an intriguing paper by Friedman et al. [41] it was demonstrated that resonant tunneling through such barriers can be seen in the hysteresis curves. The sample consisted of a powder of oriented microcrystallites fixed in an epoxy polymer matrix. The Mn_{12} clusters have $S = 10$ ground states and there is little magnetic interaction between the clusters in the crystal lattice. Thus the sample behaves as an ensemble of independent, equally oriented Mn_{12} clusters. At low temperature the magnetization of the clusters shows hysteresis curves with steps at $B_0 > 0$ when going to more positive values of the field and at $B_0 < 0$ when going to more negative values. The steps occur at well defined magnetic fields with a regular spacing of 0.46 T (see Figure 13). This macroscopic phenomenon is interpreted as

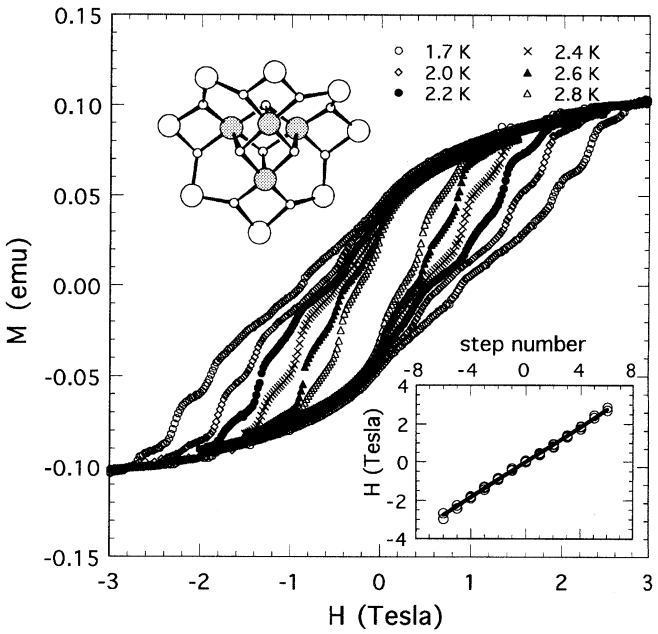

Figure 13: Magnetization of Mn_{12} as a function of magnetic field at six different temperatures (field sweep rate 67 mT/min). The inset shows the fields at which steps occur versus step number (with step 0 at zero field). The straight line is a least-squares fit, yielding a slope of 0.46 T per step. The structure of the Mn_{12} molecule is represented at the top. Only the Mn^{4+} (large shaded circles), Mn^{3+} (large open circles) and oxygen (small circles) are shown. From reference 41 with permission; copyright 1996 The American Physical Society.

resonant magnetization tunneling. The spin-spin interaction in the Mn_{12} cluster is strongly anisotropic. With the field along the molecular z-axis the spin Hamiltonian is

$$H = -D\mathbf{S_z^2} - g\beta\mathbf{SB_0} \ . \tag{21}$$

In zero field, spin states with $\mathbf{S_z} = \pm M$ are degenerate. Nevertheless the coupling between them is small and indirect transitions via states with lower $|M|$ need thermal activation since they are of higher energy due to the zero field splitting. The barrier height from $|M| = 10$ to $M = 0$ corresponds to $DS^2 = 100 \cdot D \approx 50$ cm^{-1}. If a magnetic field is applied, the $\pm M$ degeneracy of the levels is lifted and the system tends to relax to the lower part of the two spin energy wells (cf. Figure 14). If the temperature is low enough such that the activation energy needed for barrier crossing is not available, only tunneling transitions are possible that are subject to a pronounced resonance behavior. It follows from equation (21) that the resonance fields should equal $nD/g\beta$ with n an integer between 0 and 20, as has indeed been found.

An interesting property of systems like Mn_{12} is that at temperatures well below 1 K the orientation of the molecular magnetic moment must be very stable. It could therefore provide the ultimate limit for a high density magnetic memory [42].

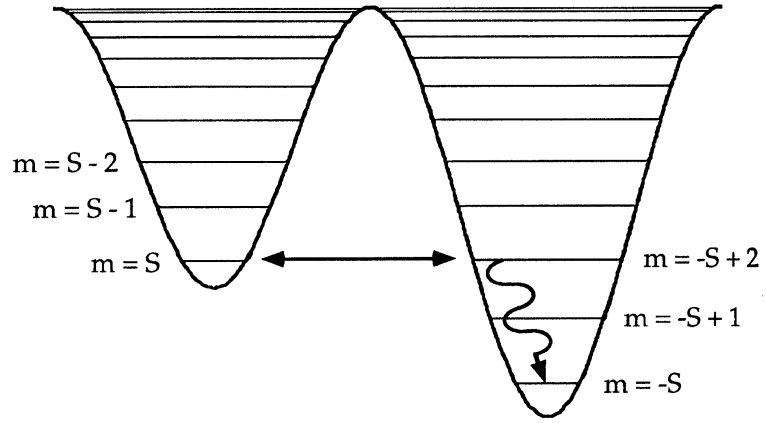

Figure 14: Schematic diagram of the resonant tunneling model. Tunneling from the metastable state $m = S$ to an excited state $m = -S + n$ is followed by a rapid spontaneous decay into the ground state. From reference 41 with permission; copyright 1996 The American Physical Society.

4 Macroscopic Forces

As outlined in the introduction, there are three types of magnetic forces: orientational and Lorentz-type in homogeneous and inhomogeneous fields and translational in inhomogeneous fields. Here we will only consider effects of homogeneous fields. If a body does not have a permanent magnetic dipole moment, its orientational energy in a magnetic field is determined by the anisotropy of its magnetic susceptibility. Assuming, for simplicity, an axially symmetric susceptibility tensor, the orientational energy only depends on the angle between the principal magnetic axis and the magnetic field:

$$E(\Theta, B_0) = -\frac{1}{2\mu_0}\left[\chi_{v,\perp} + \left(\chi_{v,\parallel} - \chi_{v,\perp}\right)\cos^2\Theta\right] {B_0}^2 \ . \tag{22}$$

Here χ_v stands for the volume susceptibility of the body. For a homogeneous body it is given by the product of the dimensionless susceptibility χ and the volume V of the body. Hence χ_v is an extensive quantity increasing linearly with the size of the body. The extremes of the function $E(\Theta, B_0)$ occuring at $\Theta = 0$ and $\Theta = 90°$ differ by

$$|\Delta E| = \frac{1}{2\mu_0}\left|\chi_{v,\parallel} - \chi_{v,\perp}\right| {B_0}^2 \equiv \Delta\chi_v {B_0}^2 \ . \tag{23}$$

orientational effects become significant only if this quantity approaches the order of kT. For $\Delta E \gg kT$ complete ordering is attained. For diamagnetic compounds, the dimensionless χ is typically of the order of 5×10^{-6}. Assuming that the typical anisotropy $\Delta\chi$ is of the same order we require a volume of 2×10^{-3} μm^3 to achieve the condition $\Delta E = kT$ at room temperature. Even for macromolecules the molecular volumes are several orders of magnitude smaller and only weak orientational effects ensue even in high fields [43]. For biological cells like erythrocytes or blood platelets the volume is approximately that size

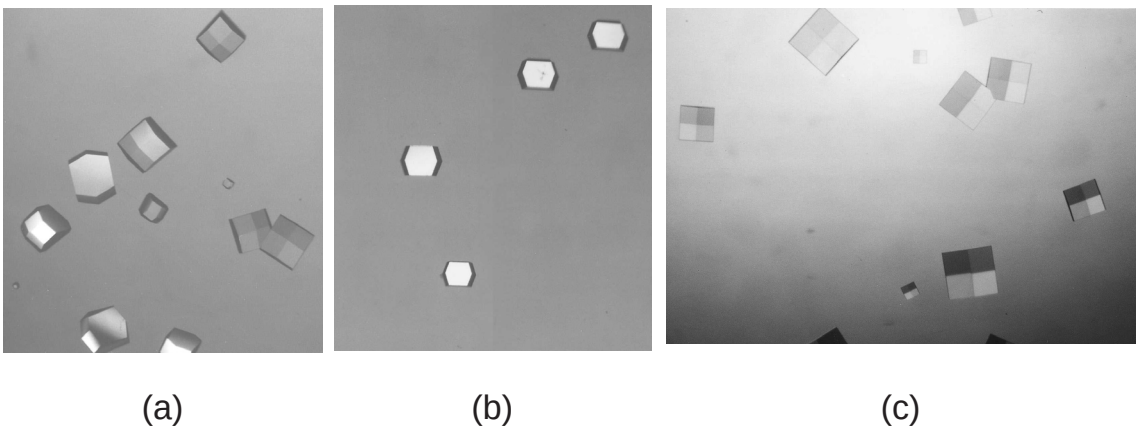

Figure 15: Magnetic orientation of crystals of hen egg-white lysozyme grown in the absence (a) and presence (b and c) of a magnetic field. The field (10 T) was applied in the left-right direction in (b) and vertically (6 T) i.e. toward the viewing axis, in (c). The *c*-axis, the unique axis of tetragonal symmetry of all the crystals is oriented along the magnetic field. As a result, {110} faces can be seen in (b) and {101} faces in (c). By contrast, the crystal orientation is random in (a). The crystals were grown at 17 °C for about 1 day from solutions containing 40 mg protein/ml and 3 % (W/v) NaCl at pH 4.6. The height of each of the photographs corresponds to a length of 2.5 mm. The experiments were performed at the Tsukuba Magnet Laboratory, National Research Institute for Metals, Japan. By courtesy of S. Sakaruzawa and M. Ataka, National Institute of Bioscience and Human Technology, Tsukuba, Japan.

and they can be well oriented in a magnetic field of 4 T [44]. Crystals of diamagnetic materials can be oriented as well if grown in a magnetic field [45]. Here the interesting question arises up to which size the crystals can reorient in the field before they settle to the bottom of the vessel. Recently, Fujiwara et al. [46] reported a study of the magnetic field dependence of the order parameter of benzophenone crystals grown in a magnetic field. Here crystal needles of about 1 cm length were formed and the order parameter was determined by visually evaluating the statistics of crystal orientations. The field dependence of the orientational distribution could be quantitatively explained by assuming a Boltzmann distribution to be established for microcrystals of 7.4×10^7 unit cells corresponding to a volume of about 0.07 μm^3. The implication was that after reaching that size the microcrystals had settled to the bottom of the vessel and their orientation was kept fixed while crystal growth went on. Thereby the distribution of the large macroscopic crystals represents an image of the orientational equilibrium distribution at a much smaller size of the crystals.

The manipulation of crystallization processes of diamagnetic materials in a magnetic field might become of practical significance in the crystallization of proteins which is a key step for their structure determination by single crystal X-ray diffraction. Thus, recent reports of oriented growth of protein crystals [47] deserve special interest. In Figure 15 we present an example observed by the group of M. Ataki. Investigations like these may indicate a very promising way for a systematic improvement of the diffraction quality of protein crystals.

References

1. cf. for example: E. Gallhuber, G. Hensler, and H. Yersin, *J. Am. Chem. Soc.* **109**, 4818 (1987)
2. P.J. Stephens, *Adv. Chem. Phys.* **35**, 197 (1975).
3. S.B. Piepho and P.N. Schatz, *Group Theory in Spectroscopy with Applications in Magnetic Circular Dichroism*, J. Wiley & Sons, New York, 1983.
4. J. Michl, *Tetrahedon* **40**, 3845 (1984)
5. E.I. Solomon, E.G. Pavel, K.E. Loeb, and C. Campchiaro, *Coord. Chem. Rev.* **144**, 369 (1995)
6. F. Neese and E.I. Solomon, *Inorg. Chem.* **38**, 1847 (1999)
7. F. Neese and E.I. Solomon *J. Am. Chem. Soc.* **120**, 12829 (1998)
8. W. Steubing, *Verh. D. Dtsch. Phys. Ges.* **15**, 1181 (1913); *Ann. Phys.* **58**, 55 (1919); *ibid.* **64**, 673 (1921).
9. J.H. VanVleck, *Phys. Rev.* **40**, 544 (1932).
10. U.E. Steiner and T. Ulrich, *Chem. Rev.* **89**, 51 (1989).
11. H. Hayashi in *Photochemistry and Photophysics*, J. F. Rabek, Ed., CRC Press, Boca Raton, 1990, Vol. I, pp. 59.
12. S. Nagakura, H. Hayashi, and T. Azumi, Eds., *Dynamic Spin Chemistry*, Kodansha, Tokyo, 1998.
13. N. Ohta, and H. Hayashi in reference 12, Chapter 4 p 118.
14. M. Yamaguchi, and I. Yamamoto in reference 12, Chapter 5 p 142.
15. T. Imamura, N. Tamai, Y. Fukuda, I. Yamazaki, S. Nagakura, H. Abe, and H. Hayashi, *Chem. Phys. Lett.* **135**, 208 (1987).
16. S. Ikeda, H. Abe, and H. Hayashi, *Chem. Phys. Lett.* **257**, 507 (1996)
17. K.M. Salikhov, Y.N. Molin, R.N. Sagdeev, and A.L. Buchachenko, *Spin Polarization and Magnetic Field Effects in Radical Reactions*, Elsevier, Amsterdam 1984.
18. U.E. Steiner and H.-J. Wolff, *Magnetic Field Effects in Photochemistry* in Photochemistry and Photophysics, J.J. Rabek and G.W. Scott, Eds., CRC Press: Boca Raton, 1991, Vol. IV, Chapter 1, pp. 1 -130.
19. H. Hayashi and S. Nagakura, *Bull. Chem. Soc. Japan* **57**, 322 (1984).
20. L. Banci, I. Bertini, and C. Luchinat, *Nuclear and Electron Relaxation*, VCH Verlagsgesellschaft, Weinheim, 1991.
21. H. Hayashi in reference 12, Chapter 2.4. p 27; K. Nishizawa, Y. Sakaguchi, H. Hayashi, H. Abe, and G. Kido, *Chem. Phys. Lett.* **267**, 505 (1997).
22. Y. Tanimoto, H. Tanaka, Y. Fujiwara, and M. Fujiwara, *J. Phys. Chem. A* **102**, 5611 (1998).
23. For a recent review see: A. Angerhofer and R. Bittl, *Photochemistry and Photobiology* **63**, 11 (1996).
24. C.E.D. Chidsey, M.G. Roelofs, and S.C. Boxer, *Chem. Phys. Lett.* **74**, 113 (1980).
25. S.G. Boxer, C.E.D. Chidsey, and M.G. Roelofs, *J. Am. Chem. Soc.* **104**, 1452 (1982).
26. S.G. Boxer in *Physical Phenomena at high Magnetic Fields, Proc. of the National High Magnetic Field Laboratory Conference, Tallahassee, Florida, 1991*, E. Manousakis,

P. Schlottmann, P. Kumar, K. Bedell, and F.M. Mueller, Eds., Addison-Wesley Publishing Company, Redwood City, 1991, pp. 437.
27. M. Wakasa, K. Nishizawa, H. Abe, G. Kido, and H. Hayashi, *J. Am. Chem. Soc.* **121**, 9191 (1999).
28. J.H. Freed in *Chemically Induced Magnetic Polarization*, L. Muus, P.W. Atkins, K.A. McLauchlan, and J.B. Pedersen, Eds., D. Reidel, Dordrecht, The Netherlands, 1977, Chapter 19.
29. J.B. Pedersen, *J. Chem. Phys.* **67**, 4097 (1977).
30. P.W. Atkins and G.T. Evans, *Mol. Phys.* **27**, 1633 (1974).
31. For a review see: K. Kalyanasundaram, *Coord. Chem. Rev.* **46**, 159 (1982)
32. D. Bürßner, H.-J. Wolff, and U.E. Steiner *Angew. Chemie Int. Ed. Engl.* **33**, 1722 (1994).
33. D. Bürßner and U.E. Steiner, unpublished results; U. Bach, Diploma Thesis, Universität Konstanz, 1995.
34. P. Gilch, F. Pöllinger-Dammer, C. Musewald, M.E. Michel-Beyerle, and U.E. Steiner, *Science* **281**, 982 (1998).
35. E.A. Guggenheim, *Thermodynamics*, 6th ed., North Holland, Amsterdam 1977, Chapter 10, pp. 333-356.
36. A.G.M. Jansen, J. Kejay, W. Wiegelamnn, P. Wyder, and W. Bronger, *Z. Physik. Chemie N.F. Munich* **182**, 9 (1993).
37. M. Yamaguchi, I. Yamamoto, T. Goto, and S. Miura, *Phys. Lett. A*. **134**, 504 (1989)
38. O. Kahn, *Molecular Magnetism*, VCH Verlagsgesellschaft, Weinheim, 1993.
39. J. Larionova, O. Kahn, S. Golhen, L. Ouahab, and R. Clérac, *Inorg. Chem* **38**, 3621 (1999).
40. R. Sessoli, D. Gatteschi, A. Caneschi, and M.A. Novak, Nature **365**, 141 (1993).
41. J.R. Friedman, M.P. Sarachik, J. Tejada, and R. Ziolo, *Phys. Rev. Lett.* **76**, 3830 (1996).
42. E.M. Chudnovsky, *Science* **274**, 938 (1996).
43. G. Maret, K. Dransfeld in *Topics in Applied Physics*, F. Herlach, Ed., Springer-Verlag, Berlin, Heidelberg, 1985, Vol. 57, pp. 143.; G. Maret, N: Boccara, J. Kiepenheuer, Eds., *Biophysical Effects of Steady Magnetic Fields*, Springer Proceedings in Physics, Springer-Verlag, Berlin, Heidelberg, 1986, Vol. 11.
44. A. Yamagishi, T. Takeuchi, T. Higashi, and M. Date, *Physica B* **177**, 523 (1992).
45. A. Katsuki, R. Tokunaga, S. Watanabe, and Y. Tanimoto, *Chem. Lett.* , 607 (1996); M. Fujiwara, T. Chidiwa, R. Tokunaga, and Y. Tanimoto, *J. Phys. Chem. B* **102**, 3417 (1998); M. Fujiwara, R. Tokunaga, and Y. Tanimoto, *ibid.* **102**, 5996 (1998).
46. M. Fujiwara, M. Fukui and Y. Tanimoto, *J. Phys. Chem. B* **103**, 2627 (1999).
47. M. Ataka, E. Katoh, I. Nobuko and N.I. Wakayama, *Cryst. Growth* **173**, 592 (1997); S. Sakurazawa, T. Kubota, and M. Ataka, *ibid.* **196**, 325 (1999); M. Ataka in *Crystallization Processes*, Wiley Series in Solution Chemistry, H. Ohtaki, Ed., Wiley, Chichester, 1998, Vol. 3, pp. 131.